EMISSION STUDIES OF ALGAE BIOFUEL WITH OXIDE NANO ADDITIVE ON THERMAL BARRIER COATED ENGINE

K.Senthil Kumar[1*], S.Karthikeyan[2], T.Dharmaprabhakaran[3], C.Thirugnanam[4]

[1*,3,4] Assistant Professor, Department of Mechanical Engineering, Syed Ammal Engineering College, Ramanathapuram, TN, India

[2]Professor, Department of Mechanical Engineering, Syed Ammal Engineering College, Ramanathapuram, TN, India

Corresponding Author: email: ksenthilme1975@gmail.com

ABSTRACT

This work deals with experimental investigations on the emission of new third-generation microalgae biodiesel-fueled internal combustion engines using esterified Nannochloropsis algae oil biodiesel fuel. The 100nm BaO (Barium oxide) of nanoparticle catalyst was added into the biodiesel fuel in YSZ coated engines. Three different test fuels like B20, B20+50ppm & B20+100ppm were prepared and tested in a diesel engine at a speed of 1500 rpm. As per ASTM standard, characterisation of all fuel was determined by evaluating physical, chemical and thermal properties. The results showed that BaO with B20 in an YSZ coated engine reduces smoke density, CO and HC emissions and also an increase in emissions of nitrogen oxide.

Keywords: Microalgae, Biodiesel, BaO, Thermal coating, Emissions.

1. Introduction

Researchers around the world have been dedicated to finding renewable energy sources. Currently, fossil fuels provide a significant proportion of the global energy demand. Biodiesel and ethanol, are therefore being developed as alternative fuels. Biodiesel can be produced from renewable sources such as vegetable oils, animal fats and recycled cooking oils. Biofuels can be classified as first generation biofuel (FGB), second generation biofuel (SGB) and third generation biofuel (TGB) based on their feedstock or production technologies. First generation biofuels are mainly sourced from food crops such as sugar cane, corn, starch and vegetable oils or animal fats. FGBs produce from food crops are limited in their ability to achieve sustainability targets for petroleum diesel substitution, environmental benefit and economic growth because of competition with their alternative uses as food products. SGBs are generally classified as being from non-edible feedstock such as wheat straw, wood and solid waste. The SGBs can avoid many of problems faced by FGBs by producing biofuels from agricultural and forest residues instead of food stocks. However, lack of available source materials in many countries may limit the potential for large-scale petroleum replacement. Microalgae may also be the only renewable source with the capacity to meet the world's transport fuel needs. This is due to high microalgae productivities and oil yield/fatty acid content compared to other oil/fatty acid-based feedstock; potentially no competition with food production; cultivation potential on non-arable and marginal land; and the production of both biodiesel and higher value coproducts. It has been estimated that microalgae biodiesel production could potentially replace petroleum diesel entirely. Microalgae may also be the only renewable source with the capacity to meet the world's transport fuel needs. (Islam et al., 2017). Moazami et al., 2012 concluded that the combining mass production of biodiesel with the higher value co-products makes microalgae an economic, renewable and carbon-neutral source of transportation biofuels, which does not compete with arable land and fresh water resource for forests and food supply. Jena et al. 2018, studied the impact of $FeCl_3$ on a CI engine. They observed an improvement in Brake Thermal Efficiency (BTE) by 8% with a decrease in CO, HC and smoke emissions, while NOx and carbon dioxide (CO_2) emissions were increased. The catalytic effect of $FeCl_3$ improved the combustion leading to increased BTE with reduced emissions. However, this improved combustion has increased the in-cylinder temperature, resulting in increased NOx emissions. The addition of metal additives has a reduction of emissions as it enables to extract comparatively higher useful work per unit fuel input. Researchers are continuously striving to get better performance from automobile engine by applying Thermal Barrier Coating (TBC) to increase the heat resistance inside the combustion chamber and offer the quantum leap in operating temperature of the internal combustion engine with durability. The present work to assess emission related problems about diesel engine with YSZ coating on piston crown and valves and the addition of BaO into the biodiesel fuel. The experimentation was conducted to represent the variation in emissions of the engine.

2. MATERIALS AND METHOD

2.1 Harvesting & Oil Extraction

Microalgal biomass harvesting can be achieved through several physicals, chemical or biological ways: flocculation, centrifugation, filtration, ultrafiltration, air flotation, auto flotation. In the centrifugation process, centrifugal forces are applied to separate algal biomass from the growth medium. After separation, the algae can be separated from the culture by simply draining the excess medium. However, the cell structure can be damaged because of high gravitational and shear forces during the centrifugation process. It is also not cost effective due to high power consumption. In mechanical extraction method, techniques such as mechanical pressing, bead milling, and homogenization are used and account for a large scale of cell disruption. Mechanic pressing puts high pressure on the cells being extracted, ruptures the cell wall, allowing the intracellular lipids to be extracted and collected. (Karthikeyan et al., 2017). The Nannochloropsis algae Biomass and Powder are shown in Figure 1.

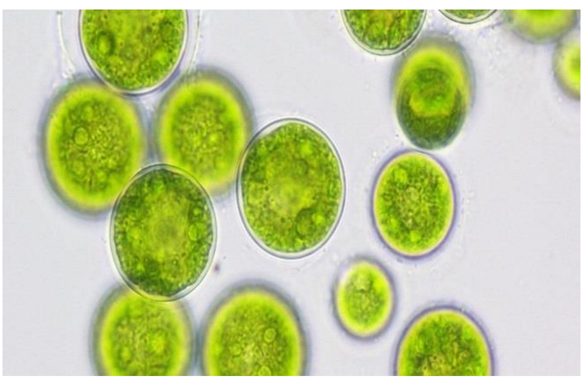

Figure 1. Nannochloropsis algae Biomass and Powder

2.2 Extraction of Biodiesel

Biodiesel is a mixture of fatty acid methyl esters obtained by transesterification of algae oil. These lipid feedstocks are composed by 90–98% per weight of triglycerides and small amounts of monoglycerides, diglycerides, free fatty acids, and residual amounts of phospholipids, tocopherols, sulphur compounds, and traces of water. Transesterification is a multiple step reaction, including three reversible steps in series, where triglycerides are converted to diglycerides, then diglycerides are converted to monoglycerides, and monoglycerides are then converted to esters (biodiesel), and glycerol (by-product). For the transesterification reaction, oil or fat and short chain alcohol (usually methanol) are used as reagents in the presence of a catalyst (like NaOH). Although the alcohol: oil theoretical molar ratio is 3:1, the molar ratio of 6:1 is generally used to complete the reaction accurately. (Sheekh et al., 2016). The Nannochloropsis algae oil biodiesel is shown in Figure 2.

Figure 2. Biodiesel Production

2.3Fourier transform infra-red analysis (FTIR)

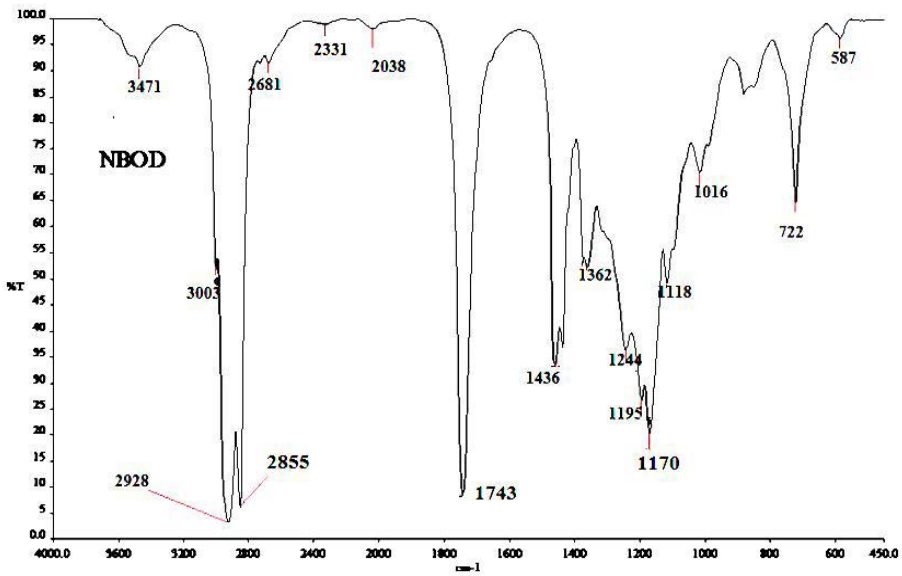

Figure 3. FTIR spectra of Nannochloropsis algae biodiesel

The FTIR spectra of Nannochloropsis algae biodiesel are shown in Figure. 3. The majority prominent is the peak at 1743 cm^{-1} (c=0 vibration) showing that this is an ester. The progress of the transesterification reaction was monitored by measuring the FTIR area under the methyl (O–CH3) peak (1,436 cm^{-1}), which accounted for the methyl esters of all types of fatty acids in the biodiesel and the strong ester peaks at 1,743 cm^{-1} (the c=0 vibration) and around 1,170 cm^{-1} (c- vibration) are clear. The observation of the peak around 1,200 cm^{-1} may be assigned to the anti-symmetric axial stretching vibration of c=c (o=o) bonds of ester while peaks around 1,183 cm^{-1} may be assigned to asymmetric axial stretching vibration of (o=cc) bonds. Since biodiesel is mainly monoalkyl ester. The intense c=o stretching bond of methyl ester appears at 1,443 cm^{-1} (Silverstein & Webstar, 1998).

2.4 Characterization of BaO Nanoparticles

The characterization of BaO nanoparticles was analysed using SEM and EDS techniques. The mean size of the BaO nanoparticles was determined by using the Scherer's equation D=K λ/β cos θ. Where K is usually taken as 0.89, D is the crystal size, λ is the wavelength of the X-ray radiation, β is the line width at maximum height, and θ is the diffraction angle. The mean size of the BaO nanoparticle was approximately 53 nm by using the above equation. SEM was used to measure the morphology and average particle size of nanoparticles. SEM image of BaO nanoparticles at a magnification of 50,000X as shown in Figure 4. The mean size of the BaO nanoparticles from SEM image varies from 40.13 to 45.54 nm. The EDS of BaO nanoparticles was shown in Figure 5. The EDS analysis confirms the presence of Ba and O in the composition of BaO nanoparticles. (Kannan and Christraj, 2018)

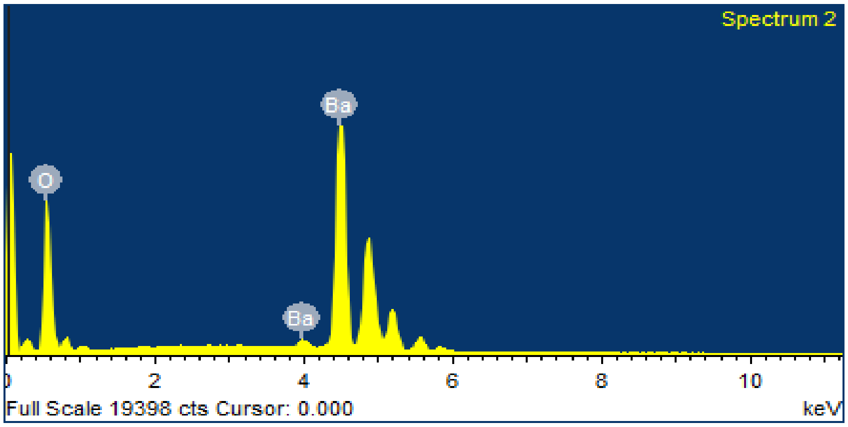

Figure 4. SEM Image of BaO nanoparticles

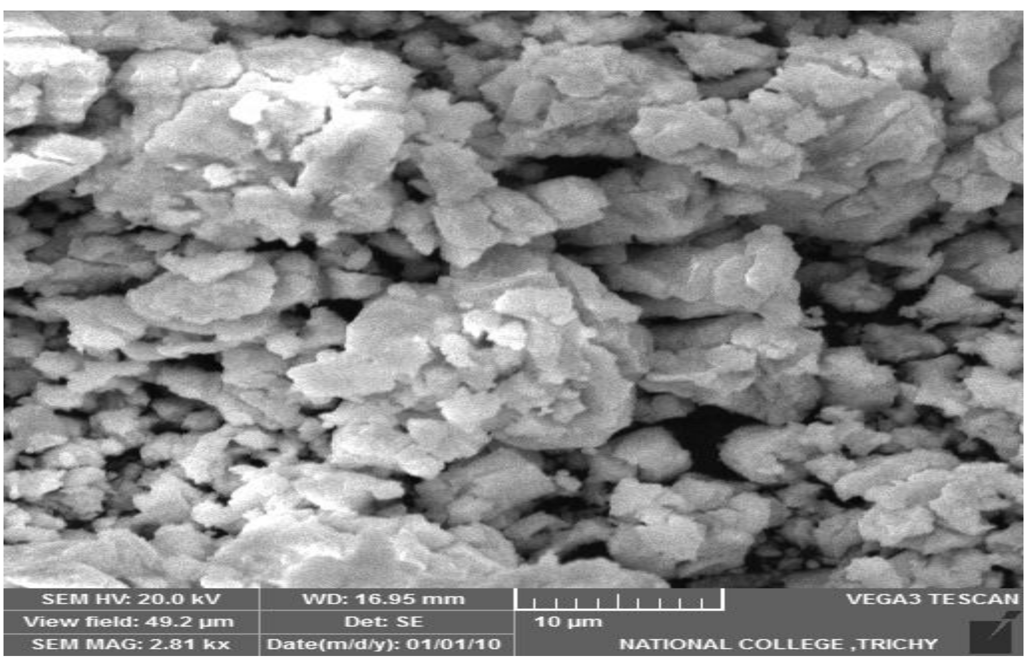

Figure 5. EDS Spectrum of BaO Nanoparticles.

2.4 Preparation of Nano blends

Figure 6. Preparation of Nano blends

The details of the nanoparticle is shown in Table 1. The BaO nanoparticles (average particle size of 50-100 nm) with a concentration of 50 ppm are weighed and dispersed into the Nannochloropsis algae biodiesel blend (B20) with the aid of an ultrasonicator. The Ultrasonication process was carried out at a frequency of 50 kHz, 120 W for 45 min duration. This process is shown in Figure 6. The prepared fuel sample was named B20+50ppm (Karthikeyan and Prathima, 2016). The same procedure is applied for the mass fraction of 100 ppm to prepare the BaO nanoparticles blended biodiesel fuel (B20+100ppm). The fuel properties of B20, B20+50ppm and B20+100ppm are determined according to the ASTM standards as shown in Table 2.

Table.1 Specification of BaO Nano particle

Formula:	BaO
Particle size	>150 nm
Product Number:	554847
CAS Number:	1304-28-5
MDL:	MFCD00003453
Formula Weight:	153.33 g/mol
Formula:	BaO
Particle size	>150 nm
Product Number:	554847
CAS Number:	1304-28-5
MDL:	MFCD00003453
Formula Weight:	153.33 g/mol

Table 2. The specifications measured based on ASTM standard for B20 and BaO blend fuels

Properties	ASTM	B20	B20+50(BaO)ppm	B20+100(BaO)ppm
Density (g/cm^3)	D-4052	0.830	0.8317	0.8317
Kinematic viscosity at 40 ˚C (mm^2/s)	D-445	4.73	5.6449	5.6894
Flashpoint (min ˚C)	D-92	176	177	178
Cloud point (˚C)	D-2500	-1	-4	-4
Pour point (˚C)	D-97	-4	-4	-4
Calorific value (kJ/kg)	D-240	43540	45483	45519
Cetane index	D-613	58	51.5	52
Water and sediment (% vol.)	D-2709	0.05	0.05	0.05

3. EXPERIMENTAL SETUP

Thermal spraying technique consists of a plasma spray method is adopted in our experimental study. To maintain the same compression ratio with the coated piston and valves, a layer of 0.5 mm thickness was removed from the top surface of both components by grinding. The piston and valve of the CI engine were sandblasted with alumina grits for mechanical interlocking of sprayed powders and bulk. A commercially available NiCrAlY powder 0.1 mm thickness bond coat was deposited by an 80 kW. Atmospheric plasma spray system on the piston and valves of CI engine using PS50 plasma torch. Then the ceramic powder 8YSZ (ZrO_2-8 wt% Y_2O_3) is sprayed on the piston crown and valves surface to form a 0.4mmthin top coat. The snapshots of uncoated baseline engine piston, valve (left) and YSZ coated piston, valve (right) are shown in Figure. 7. (Jena et al., 2018).

Single cylinder four stroke diesel engine coupled with an eddy current dynamometer is one of the commonly used engines for small, medium and high scale commercial purposes. It can withstand the peak pressure because of its large compression ratio. An experimental setup was advanced to conduct experimentations on the selected compression ignition engine with different fuel types to estimate performance and emission parameters at different operational conditions. The various components of the experimental setup are described below. The test engine used was a four-stroke, single cylinder, direct injection, water cooled and naturally aspirated CI engine. It had a bore of 87.5 mm and stroke of 110 mm. The maximum power delivered by the engine was about 5.2 KW at a constant speed of 1500 rpm and the compression ratio of 16.5:1. The suggested injection pressure and injection timings were 210 bar and 23^{o}CA bTDC, respectively (Karthikeyan and Prathima, 2016). The experimental set up is shown in Figure 8.

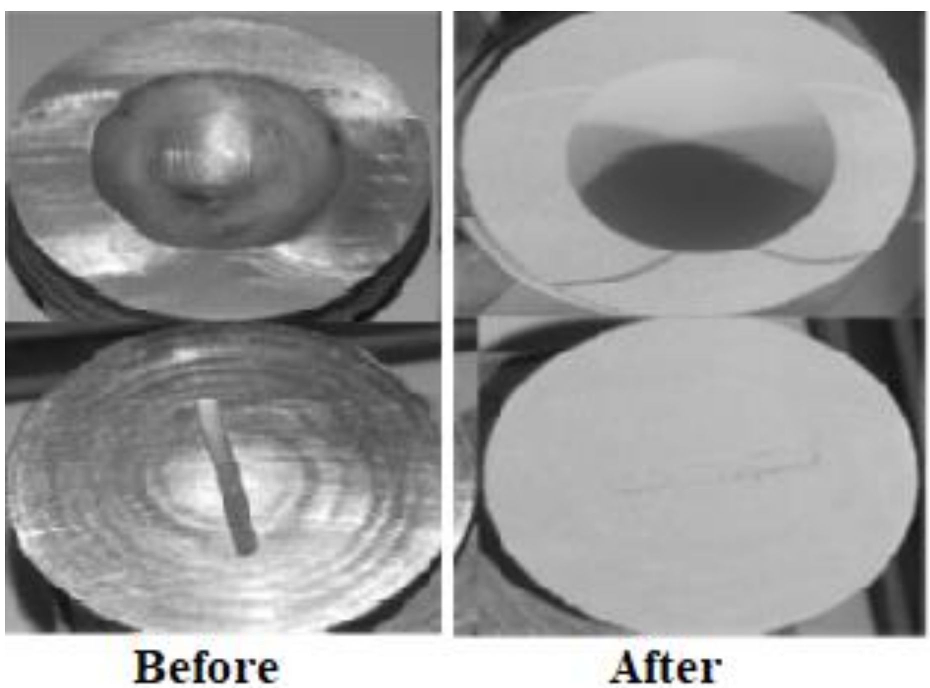

Figure. 7. Engine piston and valve coating

Figure 8. Experimental test rig.

4. RESULT AND DISCUSSION

4.1 CO Emission

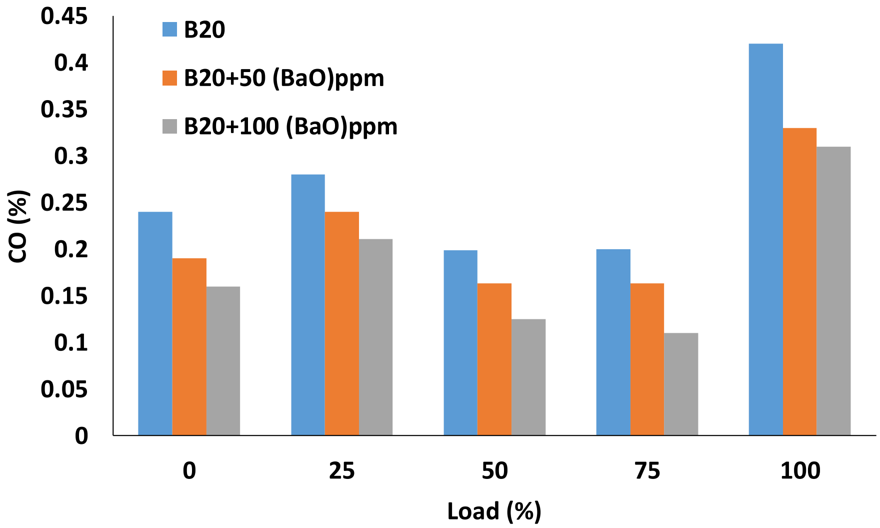

Figure 9. Variation of CO with Load

Carbon monoxide is formed during combustion due to deficiency of oxygen. It is an odourless gas but is highly toxic. On the inhalation, it is rapidly absorbed by Lungs and combines with hemoglobin in the blood-forming carboxy-hemoglobin. CO has 200 to 240 times more affinity than oxygen to combine with hemoglobin. The CO-hemoglobin complex is far more stable than oxy-hemoglobin. Thus, exposure to CO reduces the oxygen-carrying capacity of the blood to body tissues. The decrease in the supply of oxygen due to CO intoxication, damages tissues and cells and adverse effects are higher and more rapid to the brain, and the nervous system as these have higher oxygen demand. Figure 9. shows the effect of brake power on CO emissions for B20 and different blends of BaO nano additives based Biodiesel. It can be seen that the CO emission of BaO nano additives blends is less than that of B20. Predominantly, lack of oxygen was the reason for CO formation. Since BaO was an oxygenated fuel, it leads to better combustion of fuel resulting in the decrease in CO emission. This is also due to increases in combustion temperature with the increase in the engine load which is responsible for reduced CO emissions (Karthikeyan and Prathima, 2016a). Engine with TBC gives the further reduction in CO emission. As in diffusion combustion, the high temperature due to coating accelerates oxidation of CO into CO_2, which indicates improved combustion in the diesel engine due to TBC.

4.2 HC Emissions

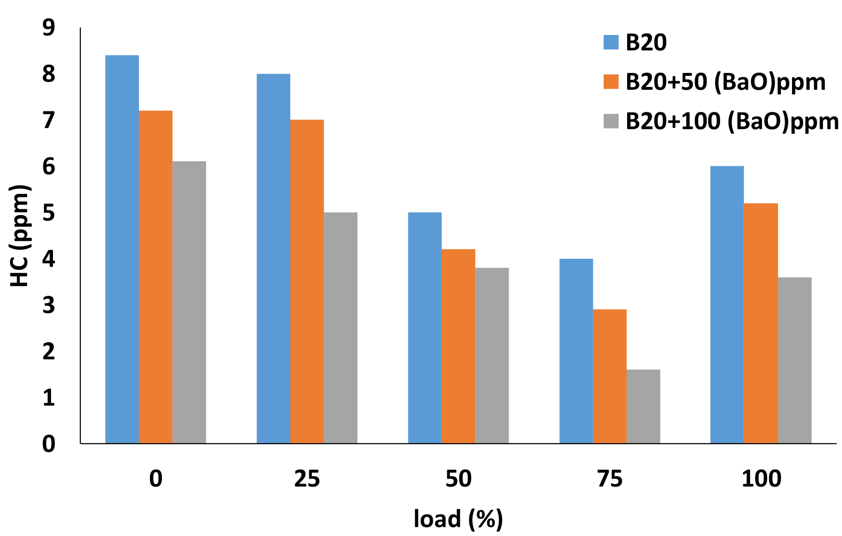

Figure 10. Variation of HC with Load

Diesel fuel has a higher boiling range and contains hydrocarbons of higher boiling and mole cell mass compared to gasoline. The unburned hydrocarbons in diesel exhaust consist of almost 400 organic compounds ranging from methane to most large fuel molecules, pyrolysis products of fuel compounds and partially oxidised hydrocarbons. In diesel engines, several events such as liquid fuel injection, fuel evaporation, fuel-air mixing, combustion and, mixing of burned and unburned gases can occur simultaneously. Figure 10. shows the effect of Load on HC emissions for B20 and its blends. Higher HC emissions were observed at low load conditions for BaO nano additives blends. This could be due to the lean mixture, the lower gas temperature that resulted due to injection of less fuel at low loads. It can also be observed HC emissions slightly decrease at medium load and significantly increase at higher load for B20 and BaO additives blends. The presence of a rich mixture at higher loads may be the reason (Karthikeyan and Prathima, 2016b). HC emission in a coated engine is reduced significantly than an uncoated engine, due to increasing in combustion temperature during afterburning phase as a consequence of the reduction in heat loss in a coated engine. As a result, the improved combustion process leads to efficient use of the intake air with improved oxidation of the supplied fuel.

4.3 NOx Emissions

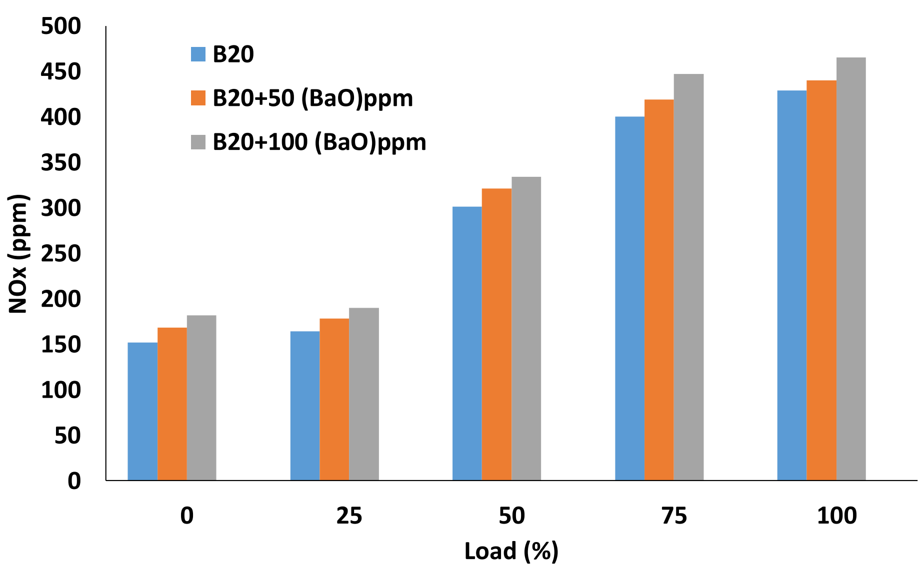

Figure 11. Variation of NOx with Load

In the Compression ignition engines, rapid combustion in pre-mixed phase is followed by diffusion combustion process. The rate at which fuel and air are mixed controls the diffusion combustion process. The reaction kinetics was leading to the formation of nitrogen oxides, and other assumptions of equilibration of the C-H-O system used in the spark ignition engines also apply to the CI Engines. As the fuel is injected in the hot compressed air, the fuel spray entrains air and non-uniform fuel distribution exists in the combustion hot compressed air, the fuel spray entrains air and non-uniform fuel distribution existed in the combustion chamber. Equivalence ratio varies widely from very rich at the core of spray to very lean at the spray boundaries. As the air is entrained into spray and spray slows down, it gets deflected more and more towards the direction of the swirl. The shape of fuel-air equivalence ratio distribution in the jet is also shown on the spray. Spray core containing fuel vapour downstream of the spray core is obtained. Ignition occurs in the slightly leaner than stoichiometric mixture region downstream of the spray core where fuel has spent the most time with the inflammable region and around stoichiometric composition burns spontaneously. In the mixing controlled phase, combustion is believed to occur in those regions of spray where the equivalence ratio is close to unity. Thus, NO is formed at varying rates depending upon the local the equivalence ratio and temperature. As the combustion progress, the already burned gases keep on mixing within colder air and fuel vapour changing its composition and temperature. The temperature of the reaction gases also changes due to compression and expansion. Figure 11. Shows the effect of load on NOx emissions for B20 and BaO blends biodiesel. It can be seen that for both the fuels, NOx emission increase. (Karthikeyan and Prathima, 2016)

4.4 Smoke opacity

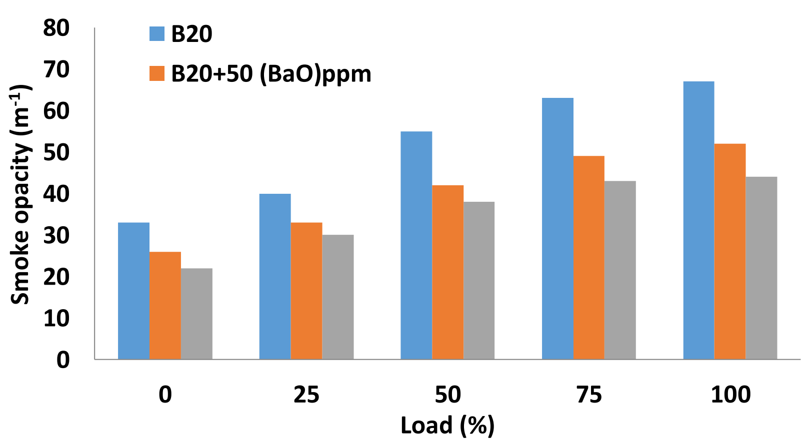

Figure 12. Variation of smoke with Load

Smoke is measured by measurement of opacity of a column or plume of exhaust gas. It is also measured by filtering a fixed volume of exhaust gases through a filter paper and the smoke stain thus formed is evaluated on the grayness scale by a reflectance meter. Particulate matter is mainly composed of soot and unburned hydrocarbons adsorbed on soot. Thus, the particulate emissions and smoke would have some correlation. For small, high-speed, turbocharged diesel engines the following correlation has some developed between Mass of PM, soot content and HC concentration. Figure 12. Shows the variation of smoke opacity with the load for B20 and BaO nano additives blends fuel. The smoke gradually increases with respect to load for all blends. It is seen from the graph that the smoke emission is lower for BaO nano blends when compared to that of B20 fuel. However, as evidence from the figure when an oxidation additive likes BaO is added to B20, it provides the favourable effect to enhance the combustion process, and the process of oxidation of the carbon to CO_2 is accelerated, and reduction of smoke opacity is evident. TBC has a positive effect on smoke emissions. (Karthikeyan and Dharma Prabhakaran, 2018).

5. CONCLUSION

From the perspective of the predicament on the energy crisis, the investigations were made using bio-fuel as alternative source of fuel. From the earlier studies, it was found that the emission characteristics of BaO bio-fuel were inferior to those of B20. Hence in this investigation TBC engine to reduce the emission characteristics. The following conclusions were drawn for the test engine based on the investigation:

- The CO and HC emissions are reduced with the addition of BaO nanoparticles blended fuel compared to the B20.
- The NOx emissions are increased with the addition of BaO nanoparticles blended fuel compared to the B20.
- The smoke opacity decreases with the addition of BaO nanoparticles blended fuel compared to the B20.

6. REFERENCES

1. Islam M. A, Heimann K, and Brown R. Microalgae biodiesel: Current status and future needs for engine performance and emissions. *Renewable and Sustainable Energy Reviews*, vol.79, pp.1160–70. (2017).
2. Jena S.P, Acharya S.K, Das H.C, Patnaik P.P and Bajpai S. Investigation of the effect of $FeCl_3$ on combustion and emission of diesel engine with thermal barrier coating. *Sustainable Environment Research,* vol. 28, pp. 72-78. (2017).
3. Kannan D, and Christraj W. Emission analysis of Azolla methyl ester with BaO nano additives for IC engine. *Energy Sources, Part A: Recovery, Utilization, and Environmental Effects,* vol.40, pp.1234–41. (2018).
4. Karthikeyan S., and Prathima A. Emission analysis of the effect of doped nano-additives on biofuel in a diesel engine. *Energy Sources, Part A: Recovery, Utilization, and Environmental Effects, vol.* 38, pp. 3702–08. (2016).
5. Karthikeyan S, and Prathima A. Emission analysis of diesel fuel using microalgae methylester with nano-La2O3. *Energy Sources, Part A: Recovery, Utilization, and Environmental Effects,* vol.38, pp.3174–80. (2016a).
6. Karthikeyan S, and Prathima A. Environmental impact of an algal biofuel doped with carbon black. *Energy Sources, Part A: Recovery, Utilization, and Environmental Effects,* vol.38, pp.3214–20. (2016b).
7. Karthikeyan S, Kalalimurugan K, and Prathima, A. Quality analysis studies on biodiesel production of neochloris oleoabundans algae. *Energy Sources, Part A: Recovery, Utilization, and Environmental Effects*, vol.40, pp.439–45. (2017).
8. Karthikeyan S, and Dharma Prabhakaran T. Emission analysis of Botryococcus braunii algal biofuel using Ni-Doped ZnO nano additives for IC engines. *Energy Sources, Part A: Recovery, Utilization, and Environmental Effects*, vol.40, pp.1060-67. (2018)
9. Moazami N, Ashori A, Ranjbar R, Tangestani M, Eghtesadi R and Nejad A.S. Large-scale biodiesel production using microalgae biomass of Nannochloropsis sp. *Biomass and Bioenergy*, vol.39, pp.449-53. (2012).
10. Sheekh M, Abomohra A.E.F and Hanelt D. Optimization of biomass and fattyacid productivity of Scenedesmus obliquus as a promising microalga for biodiesel

production. *World Journal of Microbiology and Biotechnology*, vol.29, pp.915-22. (2013).

11. Silverstein R and Webstar F. Spectrometric identification of organic compounds. 6th edition. New York: Wiley. (1998).